Received: 28 October 2021 | Revised: 17 February 2022 | Accepted: 27 March 2022

DOI: 10.1002/pen.25988

RESEARCH ARTICLE

POLYMER ENGINEERING AND SCIENCE WILEY

Smooth-rough asymmetric PLGA structure made of dip coating membrane and electrospun nanofibrous scaffolds meant to be used for guided tissue regeneration of periodontium

Paola Nitti[1] | **Barbara Palazzo**[2,3] | **Nunzia Gallo**[1] | **Francesca Scalera**[1,4] | **Alessandro Sannino**[1] | **Francesca Gervaso**[1,4]

[1]Biomaterials Laboratory, Department of Engineering for Innovation, University of Salento, Lecce

[2]Ghimas S.p.A., c/o Dhitech Scarl, Lecce, Italy

[3]ENEA Division for Sustainable Materials, Research Centre of Brindisi, Brindisi, Italy

[4]Department of Physical Sciences and Technologies of Matter, Institute of Nanotechnology-CNR, Lecce, Italy

Correspondence
Paola Nitti, Biomaterials Laboratory, Department of Engineering for Innovation, University of Salento, 73100, Lecce.
Email: paola.nitti@unisalento.it

Abstract

A surgical procedure for the repair of damaged periodontal tissue is Guided Tissue Regeneration (GTR), which involves the use of a barrier membrane to prevent soft tissue ingrowth and create a space for slow regeneration of periodontium and bone. GTR membrane should have pores able to facilitate the diffusion of fluids, oxygen, nutrients, and bioactive substances for cell growth, but also be impermeable to epithelial cells or gingival fibroblasts, which could overpopulate the defect space and inhibit infiltration and activity of bone-forming cells. In this paper, a bilayer PLGA membrane was realized by coupling the dip coating and electrospinning techniques. The rough layer of the double-sided structure was electrospun on the previously prepared smooth dip-coated membrane. A rotating drum collector at two rotating speeds was used to generate different fibers orientation. The bilayer membrane with different superimposed surfaces was successfully fabricated and characterized from a morphological, physicochemical, and the mechanical point of view. Performed analyses revealed that the membrane possesses suitable properties, especially from mechanical point of view, for its possible use as a scaffold for the GTR of periodontum. A high fiber alignment and improved mechanical properties with respect to available GTR membranes characterized the product resulting from this study.

KEYWORDS

biodegradable, biological applications of polymers, biomaterials, dental polymers, electrospinning, mechanical properties

1 | INTRODUCTION

The untreated periodontal disease such as chronic periodontitis can provoke loss of gingival tissue, connective tissue, alveolar bone, and periodontal ligaments and consequently the destruction of periodontium, and eventually tooth loss.[1] If the defect due to periodontal loss is left empty, epithelial cells and fibroblasts fill it, preventing the attachment of bone and periodontal ligament cells and so the regeneration of true periodontal tissues. Therefore, in the past few decades, the regenerative medicine and specifically, the guided tissue/bone regeneration (GTR/GBR) emerged as an alternative strategy to replace lost periodontal tissues.[2] GTR consists of the placement of a barrier membrane between the gingival epithelium and the underlying periodontal bone,[3] preventing the migration of epithelial cells or gingival fibroblasts into the defect site and promoting the growth of progenitor bone and periodontal ligament cells, which present a slower growth than fibroblasts.[4]

Ideally, a membrane for periodontal GTR should be biocompatible and biodegradable with non-toxic degradation products to avoid a second surgery for removal. Moreover, it should have cell occlusiveness, high-interconnected porosity to allow nutrients, and signaling factors diffusion, together with wastes elimination, during healing, and it should be at the same time impermeable to epithelial cells and cell-proliferative for bone cells. Furthermore, the membrane should have space maintenance ability, proper mechanical strength, and adequate clinical manageability.[5]

Membranes with such features were successfully developed (Table 1) both with biodegradable (collagen, chitosan, PLA, polyglycolic acid (PGA), and poly(lactic-*co*-glycolic acid) (PLGA)) and non-biodegradable (polytetrafluoroethylene [PTFE]) polymers and in some cases also with metals (titanium).[6,7] Recently, the use of biodegradable materials is the mainstream in GTR therapy because they allow avoiding a second surgery to remove the remaining membranes.[8]

One way to produce GTR membranes is by the electrospinning technique, which is well suited for the production of fibrous membranes in the nano range. The possibility to fabricate fibers with different orientations and size allows the electrospun scaffolds to better mimic the topology of the native extracellular matrix and to promote cell attachment and proliferation.[9] Nanofibrous membranes are particularly advantageous in GTR for their high surface area, porosity,[10] controllable degradation rate, and excellent mechanical properties[11] and because they allow fluids and nutrients to exchange through the membrane while maintaining cell occlusive porosity.

In the last years, the use of functionally graded scaffolds to fabricate biomimetic GTR membranes has emerged.[12] Using this approach, the chemical, physical and mechanical properties of each different layer can be customized to have a specific function very much similar to the natural human tissues.[12,13] In addition, the multiphasic scaffolds could allow directly the regeneration pathway, thanks to the spatial and temporal release of multiple signaling molecules that could be precisely engineered to target tissue regeneration.[14]

In this study, a membrane intended to be used for periodontium GTR was produced using PLGA, a biodegradable polymer largely used in tissue engineering because of its excellent biocompatibility, biodegradability, and mechanical strength.[15] Interestingly, PLGA nanofibers were found to be able to improve osteoblast attachment rather than PLGA bulk materials, the reason why are commonly used for dental application.[16] Based on these findings, a new bilayer membrane made with two superimposed PLGA layers was produced through the combination of two different techniques (dip-coating and electrospinning) in order to obtain two surface topographies to selectively promote or inhibit cell proliferation and migration.[11] Dip-coating technique was used to deposit a first smooth PLGA layer, on top of which a second rough PLGA layer was deposited by electrospinning. As regards the second layer, two rotating drum collector speeds were tested to generate different fibers orientation. The smooth-rough double-faced structure was manufactured to be placed with the rough surface facing the bony defect to promote the proliferation and direction migration of bone cells, while the smooth surface can be placed in contact with the gingival epithelium to prevent cell adhesion. As reported by Ribeiro et al.,[17] smooth surfaces are able to inhibit fibroblast growth, as consequence, the smooth layer produced by the dip-coating technique in our membrane should prevent cell adhesion to its flat and not porous structure. On contrary, the rough surface produced by electrospinning should improve the periodontium regeneration thanks to its nanofibrous structure that mimics native ECM, allowing cell adhesion and proliferation and facilitating the diffusion of fluids, oxygen, and

TABLE 1 Summary of the most used materials and techniques for GTR-intended membrane production

Materials	Techniques
Chitosan and hydroxyapatite (3, 13)	Freeze gelation (3), electrospinning (13)
Polylactic acid (PLA), (6, 14) Polycaprolactone (PCL) (6)	Electrospinning (6), Multilayer electrospinning (14)
Poly (lactic-*co*-glycolic acid (PLGA) (12, 19, 21)	Freeze Drying (12, 19), Electrospinning (21)
Titanium mesh (7)	

nutrients through its interconnected pores.[18] In this paper, to the best of our knowledge for the first time, it was investigated and reported the potential of the electrospinning method upon the dip-coating method to fabricate PLGA bilayer membrane, tailored to the needs of different tissues to improve wound healing/tissue regeneration in oral and maxillofacial surgery. In addition, two fiber alignment of electrospun mats were fabricated and investigated. The physiochemical characteristics of dip coated, the electrospun and bilayer membranes were evaluated. The mechanical properties of bilayer membrane were also studied, focusing on the change in mechanical properties when testing membrane with different fibers alignments.

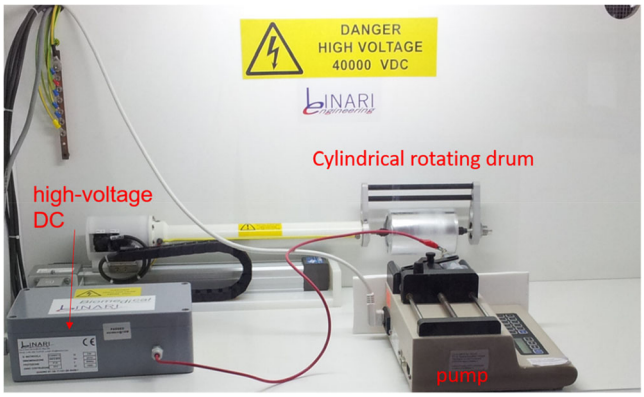

FIGURE 1 Electrospinning setup

2 | MATERIALS AND METHODS

2.1 | Materials and reagents

PLGA (Resomer RG 504, Boehringer, Germany) with a ratio of 50:50 and an intrinsic viscosity of 0.55 dL g^{-1} in $CHCl_3$ and molecular weight of 38,000–54,000 Da was used. N,N-dimethylformamide (DMF, ≥ 99,8%,) and dichloromethane (DCM ≥99,6%), selected as solvents, and phosphate buffer saline tablets (PBS) were purchased from Sigma-Aldrich (Milan, Italy). All the other used materials and reagents, of analytical grade, were purchased from the same company unless otherwise stated.

All aqueous solutions were prepared with deionized and ultrapure water (18.2 MΩ/cm, obtained by a Milli-Q® Direct Water Purification System, Merckmillipore, Darmstadt, Germany).

2.2 | Bilayer membrane fabrication

Polymer solutions for both dip-coating and electrospinning techniques were prepared using PLGA dissolved (20% wt) in a mixture (70/30) of Dichloromethane (DCM) and N,N–dimethylformamide (DMF) under magnetic stirring overnight at a room temperature to obtain homogeneous solutions.

The smooth layer of the PLGA bilayer membrane was realized by the dip-coating technique.[19] A glass substrate was cleaned with water and ethanol, dipped in the PLGA solution for 1 min and then withdrawn at a speed of 50 mm/s. The wet glass was air dried in a chemical hood for 3 days to allow slow solvents evaporation. Then PLGA film was peeled off from the glass substrate and mounted onto the drum rotating mandrel (120 mm × 30 mm) for the subsequent deposition of the PLGA rough layer by the electrospinning technique. Thus, the PLGA solution was electrospun on top of the dip-coating-produced film (dip-coated film) using a 21 G needle, a feed rate of 6 ml/h, a tip to collector distance of 10 cm, and an applied voltage of 12 kV (Figure 1). Two rotating speeds were used (100 and 2000 rpm) to generate different fibers orientation (100 rpm bilayer membrane and 2000 rpm bilayer membrane). For comparison with the bilayer membranes, also a single layer of electrospun mats was analyzed (100 rpm ES mat and 2000 rpm ES mat). The target rotation was maintained for 2 h after spinning to allow a homogeneous DCM evaporation and limit crack formation in the electrospun products.[20] All PLGA bilayer membranes and electrospun mats were then peeled off from the collector and fully characterized.

2.3 | Morphological analyses

The morphology of electrospun mats, bilayer membranes and the dip-coated film were observed by scanning electron microscopy (SEM) using an EVO® 40 (Carl Zeiss, Jena, Germany). Dried samples were coated with a 7 nm gold layer by sputtering at room temperature and examined in a variable pressure mode and with an accelerating voltage of 20 kV. Images obtained from SEM were scaled using a commercial image analysis program (ImageJ 1.50c. software, National Institute of Health, USA) in order to measure average electrospun fibers diameters and size distribution (200 measurements for each acquired sample). To evaluate relative fibers alignment in the electrospun mats at different rotation speeds, Fast Fourier Transformation (FFT) analysis was assessed using ImageJ 1.50c (NIH, USA) software.[21]

2.4 | Material water interaction

The wettability of dip-coated film, 100 and 2000 rpm electrospun mats and 100 and 2000 rpm bilayer

membranes was evaluated by measuring the static contact angle (WCA) through the sessile drop method (FTA1000 equipment, Portsmouth, VA, USA), placing a milli-Q water drop (10 µl) on the sample surface. In particular, for the bilayer membranes, the measurements were carried out on both sides of the membrane, that is, on the rough side (electrospun) and on the opposite smooth side (dip coated). At least 4 readings were performed for each specimen and results were expressed as mean value ± SD.

The water uptake ability of dip-coated film, electrospun mats, and bilayer membranes was investigated to assess their water adsorption capacity. The samples were cut in 30 × 10 mm rectangular shape and weighed (W_d) before immersion in PBS (10 mM, pH 7.4) at room temperature for 30 min, 1, 2, 5 and 24 h. After incubation, test specimens were taken out of PBS, extensively rinsed with pure water, blotted on filter paper to remove excess water and weighed again (W_w). The water uptake of samples (six samples for each group) was calculated as follows:

$$\text{Water uptake}\,(\%) = \frac{(W_w - W_d)}{W_d} \times 100, \qquad (1)$$

where W_d and W_w were specimen weights before and after immersion in PBS. Six samples for each group have been analyzed and results were expressed as mean value ± SD.

2.5 | Mechanical properties

The mechanical properties of electrospun mats and bilayer membranes were evaluated by uniaxial tensile testing and suture pull-out using a ZwickiLine universal testing machine (Zwick/Roell, Ulm, Germany) equipped with a 100 N load cell and a glass vessel filled with PBS solution to perform the test in wet condition, simulating a biological environment (Figure 5B). For both tests, scaffolds were cut into rectangles (30 × 10 mm), and soaked for 2 hs in PBS 10 mM at room temperature.

For the tensile test, each specimen ($n = 6$) was clamped 5 mm across both ends of the long side and tested following the direction along the length of the filaments with a cross-head speed of 0.1 mm/s and a preload of 0.1 N. Young's modulus (E) was calculated as the slope of the linear elastic region of the stress–strain curve at low strain values (in the range 1%–2%). Elongation at break (ε_b) and tensile strength (σ_{max}) were also evaluated. The results were expressed as average value ± SD and GraphPad Prism software (v. 8.4.2) was employed to perform statistical analysis, using one-way ANOVA analysis (p value:*≤0.05, **≤0.0001).

The suture pull-out test was performed to determine the tear strength of the membranes.[9] A single suture was made at a distance of 5 mm from the top edge and 5 mm from each side. The suture was done with a monofilament of absorbable PLGA (Polyglactin 910, VICRYL JV500) using a PS3-3/8 needle and a 5–0 gauge. The suture was left unknotted, but it was fixed to the upper claw of the mechanical test frame. Suture pullout testing ($n = 6$) of wet specimens was carried out with a 100 N load cell and an extension rate of 1 mm/min. The maximum load was recorded in Newton (N) and normalized to membrane thickness.[18] The results were expressed as average value ± SD.

3 | RESULT AND DISCUSSION

3.1 | Surface morphology of bilayer PLGA membrane

Since the aim of this study was the fabrication of a bilayer PLGA membrane intended for periodontium GTR, the confirmation of the realization of the rough PLGA electrospun layer was crucial. The concentration of PLGA solution, the solvent mixture ratio, and the electrospinning process parameters like voltage, flux, and distance between tip and collector were optimized, in order to allow producing defect-free nanofibrous matrices (Figure 2).

To obtain mats with random and aligned fibers orientation, two rotating collector speeds were used: 100 rpm for random orientation and 2000 rpm for aligned fibers. SEM images showed that fibers of the mat produced at 100 rpm rotation speed (Figure 2A) do not present a preferential direction of orientation, in comparison with mat produced at 2000 rpm speed rotation (Figure 2B) where an apparently high degree of orientation was detectable. The mean fiber diameters were 1300 and 900 nm with a SD of 400 and 300 nm for randomly orientated (100 rpm) and highly orientated (2000 rpm) fibers, respectively. Additionally, the increasing speed leads also to an increase in the number of fibers with size distribution in the range between 600 and 800 nm.

The FFT analysis of aligned and random fibers gave a clearer representation of the fiber alignment (Figure 2C–F). Random mats (100 rpm ES mats) showed a uniform distribution of fibers in all directions while aligned mats (2000 rpm ES mats) were confirmed to contain fibers with a predominant direction. 2D FFT analysis for aligned mats showed two sharp peaks of alignment at a distance of around 180° with the alignment peak value of 0.13 that indicated a higher unidirectional alignment of fibers compared to random fibers.

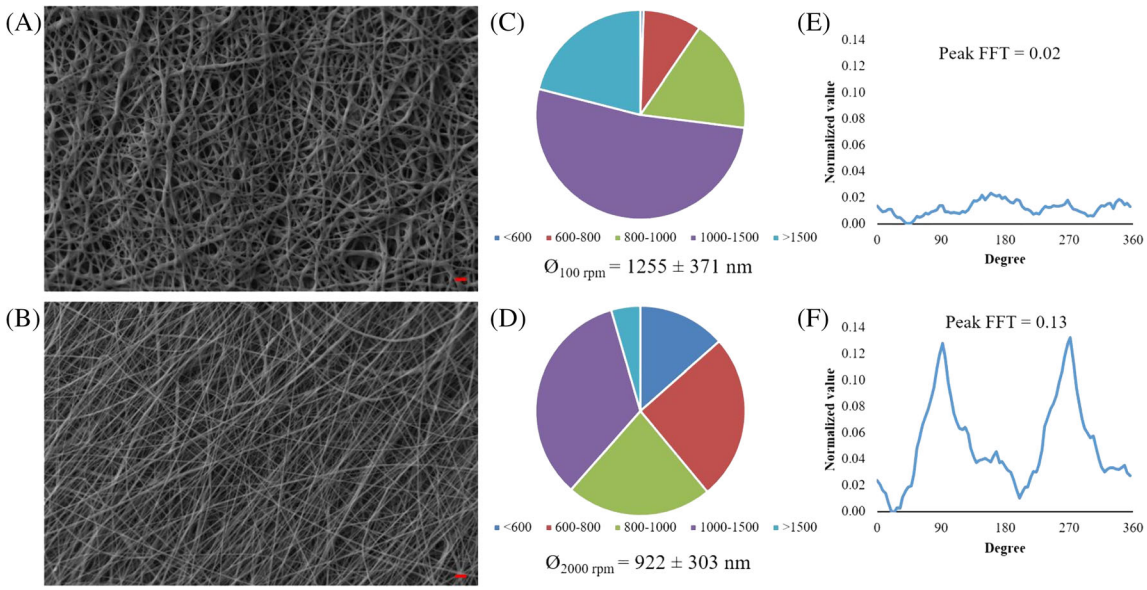

FIGURE 2 SEM micrograph of electrospun mats produced at 100 rpm (A) and 2000 rpm (B) (scale bar: 10 μm); fibers size distribution and average diameters (C, D); 2D FFT analysis (peaks of alignment at 90° and 270°) (E, F)

The smooth layer with a thickness of about 20 μm fabricated by means of the dip-coating technique and simulating the smooth side of the GTR membrane, was found to be completely flat with the absence of any porosity (data not shown), making so this membrane hypothetically impermeable to epithelial cells.

As a final step, a bilayer membrane was produced coupling dip-coating and electrospinning layers: PLGA solution was electrospun (with 100 and 2000 rpm rotating speeds) to generate random and aligned fibers orientation on the top of the previously produced PLGA film. It can be hypothesized that while the smooth layer is not adhesive to cells, the rough one should allow diffusion of fluids, oxygen, and nutrients and, thanks to its similarity to native ECM, should permit cell adhesion and proliferation. The so-obtained bilayer membranes have a thickness of about 100 μm and present a "coin-like" double face, the first one smooth (dip-coated layer) and the other one rough (electrospun layer) with topographies completely equal to those shown in Figure 2.

3.2 | Wettability analysis and water absorption ability

The hydrophilicity is one of the most important surface characteristics of biomedical materials since the scaffold chemical composition and topography influence protein absorption, cell adhesion, and proliferation.[22] Hence, both dip-coated and electrospun films (dip-coated film, 100 rpm ES mats and 2000 rpm ES mats), together with both sides of the whole membrane, (100 rpm and 2000 rpm bilayer membranes), were tested in order to determine their WCA. As shown in Figure 3A, the WCAs of both 100 and 2000 rpm electrospun mats, together with those of the rough surface present onto the bilayer membranes, were about 120° suggesting the hydrophobic behavior of these surfaces. On the contrary, the dip-coated film and the smooth surface of the bilayer matrices showed a WCA of about 75°. Those differences could be dependent on the surface morphological aspects (micro/nano-structure), as well as chemical ones (exposed functional groups). From a morphological point of view, while an ideal flat surface follows Young's model, rough surfaces with micrometric/nanometric features show very different behaviors, as described by the Wenzel and Cassie regimes or even by intermediate regimes.[23] Indeed, in a rough surface such as one of the electrospun samples (electrospun mats and rough layer of the bilayer membranes) the surface in contact with the water droplet can be very different from the projected contact area, thus strongly influencing the interfacial tension between the droplet and the sample and consequently influencing the resulting contact angle.

Since the dip-coated surfaces dip-coated film) have a WCA < 90°, from the Wenzel model the rougher surfaces resulting from the electrospun fibrous structures (ES mats and the rough side of the bilayer membranes) should have a further lower WCA. On the contrary, an increment of the WCA value was observed in the rough surfaces, in accordance with the Cassie regime, happening when air pockets are trapped under the liquid

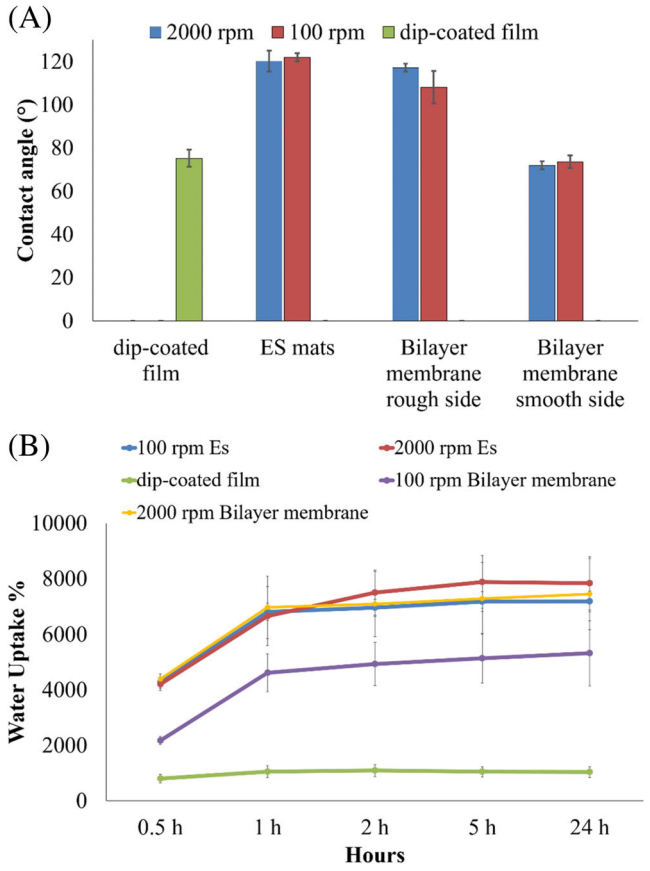

FIGURE 3 Histogram of contact angle measurement (A); water uptake tests recorded in 24 h (B)

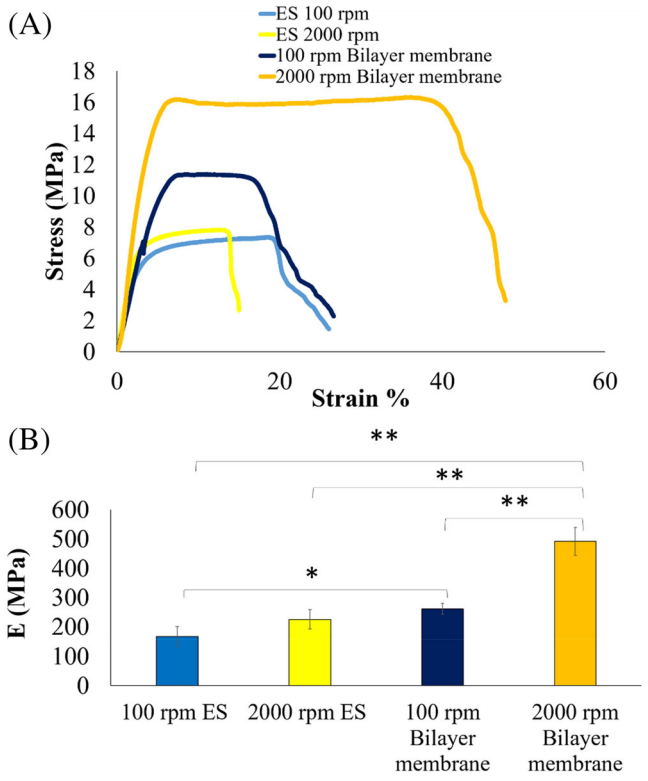

FIGURE 4 Stress–strain curves of 100 and 2000 rpm electrospun mats and 100 and 2000 rpm bilayer membranes (A); histogram of young modulus (B); (*$p < 0.05$; **$p < 0.0001$)

droplet.[24] Indeed, it is plausible that some air pockets are trapped under the water droplet when it comes in contact with the highly rough fibrous structure of the electrospun samples, thus giving rise to an increase in the contact angle.

Another important aspect of such membranes is their water absorption ability. Being the GTR membranes used in wet conditions it results are relevant to study the time in which these PLGA products are completely swelled in water. As shown in Figure 3B, although dip-coated film was less hydrophobic than the other samples as revealed by the WCA results, its capacity to absorb water is lower and remains unchanged even after 24 h of incubation. On the contrary, despite their higher hydrophobicity, the electrospun mats and the bilayer membranes present a higher water uptake than dip-coated film and attain equilibrium after 2 h. The water uptake depends mainly on the hydrophilicity of the material and the scaffold porosity. A porous material can take up and store more water whereas its nonporous counterpart can store only a limited amount of water.[25] Thus, electrospun mats and bilayer membranes behavior can be due to the intrinsic higher porosity of these samples, giving rise to a higher water absorption at longer times. In other words, looking to the previous WCA measurements, when the droplet comes in touch with the surface of the electrospun mats it presents initially a high contact angle due to air trapped, but lately, water can permeate inside the pores of the mat resulting in higher water uptake.

3.3 | Mechanical properties

Representative stress–strain plots of the tensile tests conducted on wet 100 and 200 rpm electrospun mats and onto 100 and 2000 rpm bilayer membranes are reported in Figure 4A. The stress–strain curves represent the typical mechanical behavior of this polymer.[26] The initial region up to 2% strain shows an elastic behavior of the material, in which the fibers stretch and slightly align in direction of the applied load. In the second (yielding region) and third (strain-hardening region) part of the curve, the increase of applied strain leads to a significantly increased fiber alignment and plastic deformation in mechanical behavior.

All PLGA samples present Young moduli in the order of the MPa, with the highest value reached by the bilayer

TABLE 2 Young's modulus (E), the tensile strength of 100 and 2000 rpm electrospun mats and 100 and 2000 rpm bilayer membranes

	100 rpm ES mat	2000 rpm ES mat	100 rpm bilayer membrane	2000 rpm bilayer membrane
E (MPa)	168 ± 34	226 ± 33	265 ± 19	492 ± 47
Tensile strength (MPa)	7 ± 1	6 ± 2	12 ± 1	20 ± 3
Elongation at break (%)	21 ± 8	11 ± 2	15 ± 5	45 ± 7

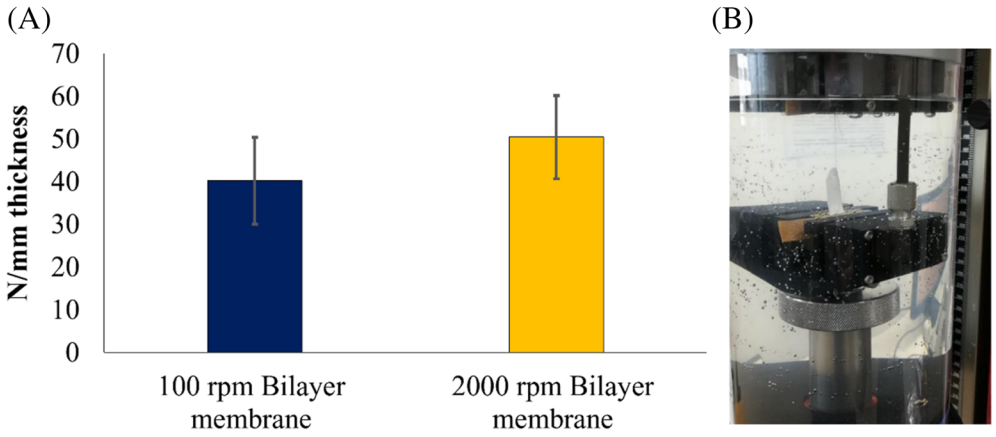

FIGURE 5 Ultimate suture pullout load normalized to membrane thickness (A); suture pullout equipment with medium container (B)

membrane produced at the collector rotation speed of 2000 rpm (Figure 4B). Table 2 summarized all the parameters obtained from the tensile tests. As expected, the 2000 rpm electrospun mats, tested in the fiber direction, exhibit a higher E modulus, equal tensile strength, and lower elongation at break values than the 100 rpm electrospun mats, although the differences are not significant (ANOVA test). The higher elongation at the break of the randomly oriented fiber mats suggests that, initially, the applied load induces the alignment of the fibers in the load direction, then, once aligned, the fibers start to resist tension. The introduction of the dip-coated film on the 100 rpm electrospun matrix significantly improved its tensile mechanical properties, inducing a significant increase in the Young modulus and tensile strength, and a significant decrease in the elongation at break. However, the combination of the dip-coated film with the 2000 rpm electrospun mats showed the highest mechanical performances, with Young modulus and tensile strength values almost double that of the single-layer mats and the elongation at the break about three times higher than other tested mats. Therefore, the presence of a dip-coated film on nanofibrous layer with highly oriented fibers significantly improved the mechanical properties of these devices.

Another aspect to consider for clinic application is the suture pullout strength. The results of the mock surgical screw-tear test on the bilayer membranes produced at 100 and 2000 rpm are shown in Figure 5 A, in which the maximum tear loads were normalized to the membrane thickness.

Specimens showed predictable tear patterns that extended upwards toward the superior edge of the specimen. Ultimate load per mm thickness measurements demonstrated bilayer high tensile tear strengths, with 40 ± 10 N mm^{-1} and 50 ± 10 N mm^{-1} for 100 rpm and 2000 rpm bilayer membranes, respectively. The strength exhibited by the PLGA bilayer membranes was higher than the commercially available GTR membranes.[9]

4 | CONCLUSION

In GTR therapy, the membrane plays a vital role that can provide a secluded space around the bone defect for osteoblast migration and growth without the interference of fibroblast or epithelial cells.[27] For this purpose, a bilayer membrane with two different surface morphologies (smooth and rough layer), one intended to be placed toward soft tissue and the other toward bone tissue was fabricated. The bilayer PLGA membrane was produced by coupling two layers, deposited by the dip-coating and electrospinning techniques. A PLGA solution was electrospun on the previously developed dip-coated membrane, rotating the drum collector at 100 and 2000 rpm speeds to generate random and aligned fibers orientation, respectively. In this way, the smooth layer produced by the dip-coating technique should conceivably prevent epithelial cells adhesion, while the rough layer produced by electrospinning can potentially improve bone regeneration.

The morphological analysis showed that dip-coated film presented a flat and non-porous structure, while both

100 and 2000 rpm electrospun layers showed a bead-free nanofibers structure. In particular, 2000 rpm electrospun mats presented higher fibers alignment and a decrease in average fibers diameters with respect to 100 rpm electrospun mats. The analysis of wettability indicated that the bilayer membranes presented high hydrophobic behavior, typical of PLGA products, while they swelled in water completely in about 2 h. Additionally, the mechanical characterization showed that the bilayer membranes, in particular those produced at 2000 rpm, have a higher Young modulus. The membrane produced in this preliminary work presented improved mechanical properties in comparison to electrospun mats and in general in comparison to commercial ones. The results of suture pullout strength on the bilayer membranes reveal that they exhibit higher strength than the commercially GTR membranes reported in literature works.

These preliminary studies demonstrated the efficacy of the novel combined electrospinning and dip coating methodology in obtaining bilayer membranes possessing adequate mechanical properties for clinical use. For this reason, it is possible to suggest the use of the developed PLGA bilayer membrane in GTR in the periodontium.

ACKNOWLEDGMENTS

This work was supported by Ghimas SPA, Casalecchio di Reno, Italy with a grant fellowship to Paola Nitti along her PhD program. The authors gratefully acknowledge Dr. Sudipto Pal and Mr. Donato Cannoletta for the assistance with the contact angle measurements and the SEM imaging, respectively. Open Access Funding provided by Universita del Salento within the CRUI-CARE Agreement.

CONFLICT OF INTEREST

The authors declare that they have no known competing financial interests or personal relationships that could have appeared to influence the work reported in this paper.

AUTHORS CONTRIBUTION

The manuscript was written through the contributions of all authors. All authors have given approval to the final version of the manuscript.

DATA AVAILABILITY STATEMENT

Data will be made available upon request to the corresponding author.

ORCID

Paola Nitti https://orcid.org/0000-0003-0333-4113

REFERENCES

[1] F. M. Chen, J. Zhang, M. Zhang, Y. An, F. Chen, Z. F. Wu, *Biomaterials* **2010**, *31*(31), 7892.

[2] K. G. Murphy, J. C. Gunsolley, *Ann. Periodontol.* **2003**, *8*(1), 266.

[3] M. C. Bottino, V. Thomas, G. Schmidt, Y. K. Vohra, T.-M. G. Chu, M. J. Kowolik, G. M. Janowski, *Dent. Mater.* **2012**, *28*(7), 703.

[4] D. Abdelaziz, A. Hefnawy, E. Al-Wakeel, A. El-Fallal, I. M. El-Sherbiny, *J. Adv. Res.* **2021**, *28*, 51.

[5] (a) Y. D. Rakhmatia, Y. Ayukawa, A. Furuhashi, K. Koyano, *J. Prosthodont. Res.* **2013**, *57*(1), 3. (b) T. V. Scantlebury, *J. Periodontol.* **1993**, *64*(11 Suppl), 1129.

[6] Y. Zhuang, K. Lin, H. Yu, *Front. Chem.* **2019**, *7*(495), 1. https://doi.org/10.3389/fchem.2019.00495

[7] H.-T. Hu, S.-Y. Lee, C.-C. Chen, Y.-C. Yang, J.-C. Yang, *Polym. Eng. Sci.* **2013**, *53*(4), 833.

[8] (a) M. Zafar, S. Najeeb, Z. Khurshid, M. Vazirzadeh, S. Zohaib, B. Najeeb, F. Sefat, *Materials (Basel, Switzerland)* **2016**, *9*(2), 73. (b) J. Wang, L. Wang, Z. Zhou, H. Lai, P. Xu, L. Liao, J. Wei, *Polymers* **2016**, *8*(4), 115. https://doi.org/10.3390/polym8040115

[9] P. A. Norowski, S. Mishra, P. C. Adatrow, W. O. Haggard, J. D. Bumgardner, *J. Biomed. Mater. Res. A* **2012**, *100*(11), 2890.

[10] S. Agarwal, J. H. Wendorff, A. Greiner, *Polymer* **2008**, *49*(26), 5603.

[11] X. Sun, C. Xu, G. Wu, Q. Ye, C. Wang, *Polymer* **2017**, *9*(6), 189.

[12] S. B. Qasim, S. Najeeb, R. M. Delaine-Smith, A. Rawlinson, I. Ur Rehman, *Dent. Mater.* **2017**, *33*(1), 71.

[13] M. C. Bottino, V. Thomas, G. M. Janowski, *Acta Biomater.* **2011**, *7*(1), 216.

[14] H. N. Woo, Y. J. Cho, S. Tarafder, C. H. Lee, *Bioactive Mater.* **2021**, *6*(10), 3328.

[15] J.-M. Lü, X. Wang, C. Marin-Muller, H. Wang, P. H. Lin, Q. Yao, C. Chen, *Exp. Rev. Mol. Diag.* **2009**, *9*(4), 325.

[16] U. Stachewicz, T. Qiao, S. C. F. Rawlinson, F. V. Almeida, W.-Q. Li, M. Cattell, A. H. Barber, *Acta Biomater.* **2015**, *27*, 88.

[17] C. Ribeiro, V. Sencadas, A. C. Areias, F. M. Gama, S. Lanceros-Méndez, *J. Biomed. Mater. Res. Part A* **2015**, *103*(7), 2260.

[18] I. Yoshimoto, J.-I. Sasaki, R. Tsuboi, S. Yamaguchi, H. Kitagawa, S. Imazato, *Dent. Mater.* **2018**, *34*(3), 538.

[19] S. Attia, J. Wang, G. M. Wu, J. Shen, J. H. Ma, *J. Mater. Sci. Technol.* **2002**, *18*, 211.

[20] D. M. Campos, K. Gritsch, V. Salles, G. N. Attik, B. Grosgogeat, *BioRes. Open Access* **2014**, *3*(3), 117.

[21] (a) C. Ayres, G. L. Bowlin, S. C. Henderson, L. Taylor, J. Shultz, J. Alexander, T. A. Telemeco, D. G. Simpson, *Biomaterials* **2006**, *27*(32), 5524. (b) P. Nitti, N. Gallo, L. Natta, F. Scalera, B. Palazzo, A. Sannino, F. Gervaso, *J. Healthc. Eng.* **2018**, *2018*, 3651480. https://doi.org/10.1155/2018/3651480

[22] A. D. Li, Z. Z. Sun, M. Zhou, X. X. Xu, J. Y. Ma, W. Zheng, H. M. Zhou, L. Li, Y. F. Zheng, *Colloids Surf., B* **2013**, *102*, 674.

[23] D. Liviu, A. Popescu, I. Zgura, N. Preda, I. Mihailescu, Wettability of Nanostructured Surfaces. in *Wetting and Wettability* (Ed: M. Aliofkhazraei), InTech, London, UK **2015**, p. 207.

[24] P. Nitti, N. Gallo, B. Palazzo, A. Sannino, A. Polini, T. Verri, A. Barca, F. Gervaso, *Polym. Test.* **2020**, *91*, 106758. https://doi.org/10.1016/j.polymertesting.2020.106758

[25] N. Sultana, M. Wang, Water Uptake and Diffusion in PHBV Tissue Engineering Scaffolds and Non-porous Thin Films. in *International Conference on Biomedical*

Engineering and Technology IPCBE, Vol. 11, IACSIT Press, Sinapore **2011**.

[26] S.-F. Chou, K. A. Woodrow, *J. Mech. Behav. Biomed. Mater.* **2017**, *65*, 724.

[27] J. Behring, R. Junker, X. F. Walboomers, B. Chessnut, J. A. Jansen, *Odontology* **2008**, *96*(1), 1.

How to cite this article: P. Nitti, B. Palazzo, N. Gallo, F. Scalera, A. Sannino, F. Gervaso, *Polym. Eng. Sci.* **2022**, *62*(6), 2061. https://doi.org/10.1002/pen.25988